JAERI 1253

JAERI 1253

FEMRZ

Program for Solving Two-Dimensional Neutron Transport Problems in Cylindrical Geometry by the Finite Element Method

February 1978

日 本 原 子 力 研 究 所

Japan Atomic Energy Research Institute

JAERI レポート

この報告書は，日本原子力研究所で行なわれた研究および技術の成果を研究成果編集委員会の審査を経て，不定期に刊行しているものです．

入手（資料交換による），複製などのお問合わせは，日本原子力研究所技術情報部（〒319-11 茨城県那珂郡東海村）あて，お申しこみください．なお，このほかに財団法人原子力弘済会情報サービス事業部（茨城県那珂郡東海村日本原子力研究所内）で複写による実費頒布をおこなっております．

JAERI Report

Published by the Japan Atomic Energy Research Institute

Inquiries about the availability of reports and their reproduction should be addressed to the Division of Techinical Information, Japan Atomic Energy Research Institute, Tokai-mura, Naka-gun, Ibaraki-ken, Japan.

編集兼発行　日本原子力研究所
印　　刷　株式会社小薬印刷所

JAERI 1253

FEMRZ

Program for Solving Two-Dimensional Neutron Transport Problems in Cylindrical Geometry by the Finite Element Method

Toichiro FUJIMURA, Tsuneo TSUTSUI, Kunihiko HORIKAMI,
Tadahiro OHNISHI* and Yasuaki NAKAHARA

Division of Reactor Engineering, Tokai Reseach Establishment,
Japan Atomic Energy Research Institute, Tokai-mura, Naka-gun, Ibaraki-ken

Received July 15, 1977

A computer program based on the finite element method has been developed for solving multi-group neutron transport problems in two-dimensional cylindrical (r, z) geometry. In the solution algorithm, the method of higher order finite elements has been applied to the spatial variables on rectangular (r,z) subregions. It is based on the discontinuous method with Galerkin-type scheme.

Some calculational examples are given for a guide to practical applications. The results and discussions are given in comparison with the S_n method to illustrate the effectiveness of FEMRZ. It is seen that FEMRZ solutions obtained from the biquadratic approximation are accurate and stable enough even for the considerably coarse meshes.

KEYWORDS: Finite Element Method, Neutron Transport, Cylindrical Geometry, Higher Order Approximation, Galerkin-type Scheme, Discontinuous Method, Coarse Mesh Rebalance, Code Manual, Discrete Ordinate Method.

* Atomic Energy Research Laboratory, Hitachi, Ltd.

FEMRZ

二次元円柱体系における中性子輸送問題を有限要素法で解くプログラム

日本原子力研究所東海研究所原子炉工学部

藤村統一郎，筒井恒夫，堀上邦彦，大西忠博*，中原康明

1977年7月15日受理

有限要素法により，二次元 (r, z) 円柱体系における多群中性子輸送問題を解くプログラムを開発した．数値解法としては，高次近似の有限要素法が長方形の (r, z) 小領域上の空間変数に対し，ガレルキン法を用いた不連続法に基づいて適用されている．

実際の応用の便宜のためにいくつかの計算例が与えられ，その結果が FEMRZ の有効性を例証するために S_n 法と比較され検討されている．双二次近似による解は，かなり粗いメッシュのときでも十分精度が良く，数値的にも安定である．

* 日立製作所　原子力研究所

Contents

目　　次

1. Introduction

The FEM (the Finite Element Method) was originated in early times in the field of structure analysis,[1] but its application to technical or mathematical fields other than structure analysis has only a short history. Nowadays, the FEM are applied extensively for solving problems in many fields because of its geometrical flexibility in applications and stability in numerical calculations.[2] It has been applied also to the reactor physics calculations since 1971.[3]

In the neutron transport calculations, many numerical methods have been proposed, but it is notable that the finite difference discrete ordinate method (the so-called S_n method) has occupied a dominant position in practical applications to multi-group and multi-region reactor core analyses. Experiences on the S_n method have proved its excellent usefulness, but mathematical foundations for its general application to complicated geometries have not yet been established. The S_n method may sometimes fail to give uniform convergence in iterative solutions for some sensitive problems.[4]

The application of the FEM to a space spanned with spatial variables seems to have following advantages over the S_n method ;[5]

1) Any higher order approximation of arbitrary basis functions can be applied.
2) Any complex geometrical configurations can be simulated accurately.[3]
3) A reliable mathematical foundation has been established on the Ritz-Galerkin variational principle[2] adopted in the FEM.

In contrast to the S_n method, the FEM has been tried for solving transport problems only in academic circles and is not yet popular partly because of its somewhat tedious formulation. The FEM, however, still in its infancy in reactor physics, has great possibilities to grow to a powerful tool in reactor analyses and designs. Since only the case of one-dimensional[6] and two-dimensional planar geometries[4,7] have been treated as yet, we have developed an FEM algorithm in (r,z) geometry.[8] Our work is also supported by the fact that most of the two-dimensional core analyses are of (r,z) geometry.

Main features of the algorithm are as follows:

1) Discrete ordinate S_n approximation is used for angular variables. (Application of the FEM to the angular space is feasible. However, this may not be advantageous because of introducing additional complexities into the algorithm.)
2) The whole system is divided into a number of axisymmetric tori with rectangular cross sections in (r,z) plane.
3) Four and nine nodes are allocated for a subregion as shown in Fig. 1, corresponding to bilinear and biquadratic approximation, respectively. (Other higher order approximations are not practical since they require so much computing cost.[8])
4) Spatial distribution of the angular flux in a subregion is represented as a linear combination of Lagrange's interpolating polynomials, coefficients of which are matched with nodal values of the fluxes.
5) The discontinuous method which allows discontinuity of the flux at the boundaries of a subregion is used. (It has been indicated in Ref. 4) that the continuous method

may bring about numerical instability caused by negative fluxes.)

6) Galerkin-type scheme is adopted to eliminate the residual. (Lagrange's interpolating polynomials are well-conditioned on the linear independency and the choice of the same weight function as the basis function simplifies the computations of inner products.[9])
7) The resulting algebraic matrix equations are solved by the no-pivoting Crout's method.[10]
8) No recipe for negative fluxes is introduced. (Negative flux appearance being peculiar to the finite difference method, S_n programs have a "set-negative-flux-to-zero" recipe.[12] The FEM, on the other hand, does not need it.)
9) Space and angle variables are swept along the neutron flight direction to evaluate the angular flux.
10) Iterations are accelerated by using a coarse mesh rebalance method[11] in which the rebalance coarse meshes can arbitrarily be set up.

(a) For bilinear approximation (b) For biquadratic approximation

Fig. 1 Node arrangements in a subregion for bilinear and biquadratic approximations.

The code FEMRZ has been developed by using these algorithms on the FACOM 230-75 computer. It can, however, easily be converted to the other computers because of the use of the standard FORTRAN. For the convenience of the programing, the FEMRZ is formed in a structure very much similar to the diamond difference S_n code TWOTRAN-II,[12] but the method of solution is considerably different on account of having used the FEM as shown in the next chapter. The program informations for users and discussions about some illustrative examples are given in Chapters 3 and 4, respectively.

2. Method of Solution

For the convenience of readers, the same notations and angular coordinate system as those in Ref. 12) are used. The coordinate system is shown in Fig. 2 and the notations are listed below.

Ω	velocity direction of particle
μ,η,ξ	direction cosines of Ω
ω	horizontal angle of Ω
φ	azimutal angle of Ω
g	index of discretized energy
m	index of discretized angle
ΔE_g	g-th energy interval
$\Delta\Omega_m$	m-th element of solid angle about Ω
σ_t	macroscopic total cross section
σ_s	macroscopic scattering cross section
σ_f	macroscopic fission cross section
ν	numder of particles emitted isotropically per fission
χ_g	fraction of emitted particles liberated in g-th energy interval

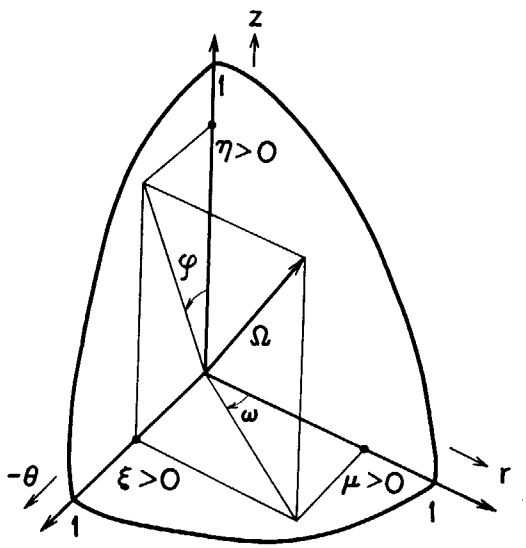

Fig. 2 Angular coordinate system in (r,z) geometry.

2. 1 Energy and angular discretizations

The time-independent two-dimensional transport equation in (r,z) geometry is written as follows;

$$\frac{\mu}{r}\frac{\partial(r\psi^g)}{\partial r}-\frac{1}{r}\frac{\partial(\xi\psi^g)}{\partial\omega}+\eta\frac{\partial\psi^g}{\partial z}+\sigma_t^g\psi^g=S^g,\quad (g=1\sim IGM^*), \tag{1}$$

* The meanings of FORTRAN variables are give in TABLE 1 or 3.

where

$$\psi^g = \int_{\Delta E_g} \psi(r, z, \mu, \varphi, E)dE.$$

By the assumption of the φ-symmetry of the angular flux ψ, Eq. (1) in the S_n approximation on the angular space leads to

$$w_m\mu_m \frac{1}{r}\frac{\partial(r\psi_m^g)}{\partial r} + w_m\eta_m\frac{\partial\psi_m^g}{\partial z} + \frac{1}{r}(\alpha_{m+1/2}\psi_{m+1/2}^g - \alpha_{m-1/2}\psi_{m-1/2}^g)$$

$$+ \sigma_t^g w_m\psi_m^g = w_m S_m^g, \quad (g=1\sim IGM,\ m=1\sim MMT), \tag{2}$$

where the unit angular sphere is partitioned into $2\times MMT$ sections. Quantities with angular suffices are given by

$$w_m = \iint_{\Delta\Omega_m} d\mu d\varphi/2\pi,$$

$$\psi_m^g = \left[\iint_{\Delta\Omega_m} \psi^g d\mu d\varphi/2\pi\right] \Big/ w_m,$$

$$\alpha_{m+1/2} = \alpha_{m-1/2} - w_m\mu_m,$$

respectively, and the initial values $\alpha_{m-1/2}$ vanish on each η level (see Fig. 3).

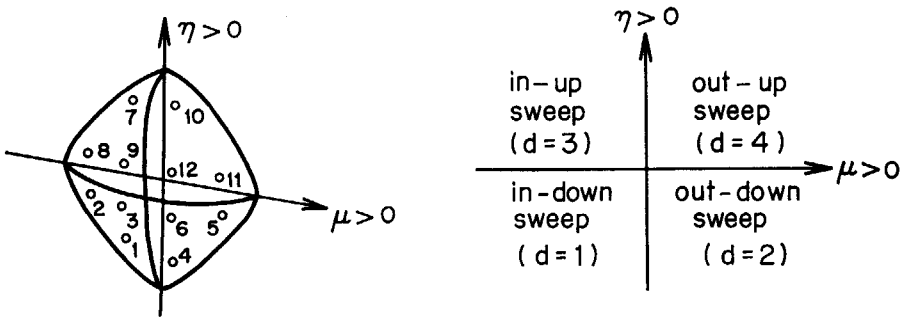

(a) Sweep through angular suffix (b) Sweep through direction

Fig. 3 Order of sweeps through the angular suffix m (for $MMT=12$) and the direction d.

2. 2 Flux and source approximations

In each rectangular subregion with NPT nodes (see Fig. 1), the NP-th order Lagrange's interpolating polynomial $L^l=L^l(r,z)$ is defined so that it takes the value unity at the l-th node and zero at all other nodes. Using these polynomials, we can give an approximate expression $\tilde{\psi}_m^g(r,z)$ to the unknown $\psi_m^g(r,z)$ in Eq. (2) with the following linear combination:

$$\tilde{\psi}_m^g = \sum_{l=1}^{NPT} \psi_m^{gl} L^l,$$

where the coefficient ψ_m^{gl} can be interpreted as the value of the angular flux at the l-th node. We show only the local expression for the subregion for simplicity, but the global expression can be derived easily.

Next, we approximate the source term $S_m^g(r,z)$ in Eq. (2) where it is treated as known. For this purpose, let us define the nodal flux components (the coefficients in spherical harmonics expansion of the angular flux) as

$$\phi_{nk}^{gl} = \sum_{m=1}^{MMT} w_m R_{nk}^m \psi_m^{gl}, \quad (k=0\sim n,\ n=1\sim ISCT),$$

using the spherical harmonics R_{nk} (μ_m, φ_m) of n-th order. This means that the flux components :

$$\phi_{nk}^g = \int_{-1}^{1} d\mu \int_0^{\pi} d\varphi R_{nk}(\mu, \varphi)\psi^g/2\pi$$

are approximated by

$$\tilde{\phi}_{nk}^g = \sum_{l=1}^{NPT} \phi_{nk}^{gl} L^l.$$

Assuming the neutron cross sections are constant in the subregion, the nodal source components are represented as follows:

$$S_{nk}^{gl} = \sum_{g'=1}^{ISCT} (2n+1)\sigma_{sn}^{g'\to g}\phi_{nk}^{g'l} + \chi_g \sum_{g'=1}^{IGM} \nu\sigma_f^{g'}\phi_{00}^{g'l} + (2n+1)Q_{nk}^{gl}, \tag{3}$$

$(g=1\sim IGM,\ l=1\sim NPT)$,

where the Q_{nk}^{gl}'s are also the nodal values of the external source components. As we keep the flux components instead of the angular flux to save the computer core storage, the source term is given by

$$S_m^g = \sum_{n=0}^{ISCT} \sum_{k=0}^{n} R_{nk}^m \sum_{l=1}^{NPT} S_{nk}^{gl} L^l, \quad (g=1\sim IGM,\ m=1\sim MMT).$$

2. 3 Discontinuous method

This method can be compared with the discontinuous method formulated in TRIPLET.[4] The sweeping orders of space and angular meshes are simslar to those of TWOTRAN-II.

In the beginning, let us consider a subregion;

$$D_{ij} = \{(r, z) | r_{i-1/2} \leqq r \leqq r_{i+1/2},\ z_{j-1/2} \leqq z \leqq z_{j+1/2}\}$$

which belongs to the i-th interval in the r-direction and the j-th interval in the z-direction. Let L, R, B and T be the sets formed from the nodes which belong to the left, right, bottom and top boundaries of the D_{ij}, respectively. Then, two kinds of Lagrange's interpolating polynomials of one variable are constructed from the function L^l as follows:

$$L_r^l = \begin{cases} L^l(r, z_{j-1/2}) & if\ l\in B, \\ L^l(r, z_{j+1/2}) & if\ l\in T, \end{cases}$$

and

$$L_z^l = \begin{cases} L^l(r_{i-1/2}, z) & if\ l\in L, \\ L^l(r_{i+1/2}, z) & if\ l\in R. \end{cases}$$

With the above notations, we define the following three kinds of inner products in the D_{ij};

$$\langle f, g\rangle = \begin{cases} \iint_{D_{ij}} fgrdrdz, & if\ f\cdot g\ is\ a\ function\ of\ r\ and\ z, \\ \int_{r_{i-1/2}}^{r_{i+1/2}} fgrdr, & if\ f\cdot g\ is\ a\ function\ of\ r, \\ \int_{z_{j-1/2}}^{z_{j+1/2}} fgdz, & if\ f\cdot g\ is\ a\ function\ of\ z. \end{cases}$$

The following nine inner products are sufficient for the discontinuous method using the Galerkin-type scheme.[2]

$$\langle 1, L^l\rangle,\ \langle L^{l'}, L^l\rangle,\ \langle L^{l'}, \frac{1}{r}L^l\rangle,\ \langle L^{l'}, \frac{\partial}{\partial r}L^l\rangle,\ \langle L^{l'}, \frac{\partial}{\partial z}L^l\rangle,$$

$$\langle 1, L_r^l\rangle,\ \langle L_r^{l'}, L_r^l\rangle,\ \langle 1, L_z^l\rangle,\ \langle L_z^{l'}, L_z^l\rangle.$$

In addition, we can simplify the calculations of the inner products with the help of, for instance, the following relations:[8]

$$\langle L^{l'}, L^l\rangle = \langle L^l, L^{l'}\rangle, \text{ for any pair of } (l', l),$$

$$L_i^{l'} = L_i^l, \text{ for facing nodes } (r_{i-1/2}, z_{l'}) \text{ and } (r_{i+1/2}, z_l).$$

Now, by using the condition:

$$\psi_m^{gl} = \psi_{m-1/2}^{gl}, \quad (l=1\sim NPT),$$

for the initial angular mesh of the sweep in each η level and the relation:

$$\psi_{m+1/2}^{gl} = 2\psi_m^{gl} - \psi_{m-1/2}^{gl}, \quad (l=1\sim NPT),$$

the residual $R_m^g(r,z)$ of Eq. (2) is defined as follows:

$$\begin{aligned}
R_m^g = {} & w_m|\mu_m|r_{i+1/2}\Big[\sum_{l\in R}(\psi_m^{gl}-\psi_m^{g\bar{l}})\Big]L_i^l(\delta_{d1}+\delta_{d3}) + w_m|\eta_m|\Big[\sum_{l\in T}(\psi_m^{gl}-\psi_m^{g\bar{l}})\Big]L_r^l(\delta_{d1}+\delta_{d2}) \\
& + w_m|\mu_m|r_{i-1/2}\Big[\sum_{l\in L}(\psi_m^{gl}-\psi_m^{g\bar{l}})\Big]L_i^l(\delta_{d2}+\delta_{d4}) + w_m|\eta_m|\Big[\sum_{l\in B}(\psi_m^{gl}-\psi_m^{g\bar{l}})\Big]L_r^l(\delta_{d3}+\delta_{d4}) \\
& + w_m\mu_m\sum_{l=1}^{NPT}\psi_m^{gl}\left(\frac{\partial}{\partial r}L^l\right) + w_m\eta_m\sum_{l=1}^{NPT}\psi_m^{gl}\left(\frac{\partial}{\partial z}L^l\right) + (\alpha_{m+1/2}+\alpha_{m-1/2})\sum_{l=1}^{NPT}\psi_m^{gl}\left(\frac{1}{r}L^l\right) \\
& + \sigma_t^g w_m\sum_{l=1}^{NPT}\psi_m^{gl}L^l - (\alpha_{m+1/2}+\alpha_{m-1/2})\sum_{l=1}^{NPT}\psi_{m-1/2}^{gl}\left(\frac{1}{r}L^l\right) - w_m S_m^g, \\
& (g=1\sim IGM,\ m=1\sim MMT).
\end{aligned}$$

The $\delta_{dd'}$'s are the Kronecker's deltas in which d refers to a direction of the sweeps as shown in Fig. 2 and $(\psi_m^{gl}-\psi_m^{g\bar{l}})$ is the difference between inside and outside values of the angular flux at the same point on the boundary of the subregion D_{ij}. The flux discrepancy is peculiar to the discontinuous method, which, however, can avoid over-fitting of the approximate solutions, so that ensure a good stability. The residual contains NPT unknowns ψ_m^{gl} for the fixed suffices g, i, j and m, if we assume the values $\psi_{m-1/2}^{gl}$ and $\psi_m^{g\bar{l}}$ to be known.

Thus, the Galerkin's method

$$\langle L^{l'}, R_m^g\rangle = 0, \quad (l'=1\sim NPT), \tag{4}$$

can be applied to yield the equations of the unknowns.

This situation can be compared with that of TWOTRAN-II,[12] which is based on a continuous method. The residual is given by

$$\begin{aligned}
& w_m\mu_m\frac{2}{(r_{i+1/2}+r_{i-1/2})}\left(\frac{r_{i+1/2}}{r_{i+1/2}+r_{i-1/2}}\psi_m^{gR} - \frac{r_{i-1/2}}{r_{i+1/2}-r_{i-1/2}}\psi_m^{gL} - \psi_m^{gD}\right) \\
& + w_m\eta_m\frac{1}{(z_{j+1/2}-z_{j-1/2})}(\psi_m^{gT}-\psi_m^{gB}) + (\alpha_{m+1/2}+\alpha_{m-1/2})\frac{2}{(r_{i+1/2}+r_{i-1/2})}\psi_m^{gD} \\
& + \sigma_t^g w_m\psi_m^{gD} + (\alpha_{m+1/2}+\alpha_{m-1/2})\frac{2}{(r_{i+1/2}+r_{i-1/2})}\psi_{m-1/2}^{gD} - w_m\Big(\sum_{n=0}^{ISCT}\sum_{k=0}^{n}R_{nk}S_{nk}^{gD}\Big),
\end{aligned}$$

where ψ_m^{gD}, ψ_m^{gL}, ψ_m^{gR}, ψ_m^{gB}, ψ_m^{gT}, $\psi_{m-1/2}^{gD}$ and S_{nk}^{gD} stand averages of ψ_m^g over the subregion D_{ij}, its left boundary, right boundary, bottom boundary and top bounbary, and averages of $\psi_{m-1/2}^g$ anb S_{nk}^g over D_{ij}, respectivery. If one of directions of the sweep is assumed, the two of bounbary fluxes are regarded as knowns, and the diamond difference equations;

$$2\psi_m^{gD} = \psi_m^{gL} + \psi_m^{gR},$$

$$2\psi_m^{gD} = \psi_m^{gB} + \psi_m^{gT}$$

lead to a single equation with only one unknown of ψ_m^{gD}.

For the present case, after dividing Eq. (4) by w_m, we have a linear system of equations as follows:

$$\boldsymbol{A}\boldsymbol{\phi} = \boldsymbol{b}, \tag{5}$$

where the explicit expressions of the matrix $\boldsymbol{A}=(a_{l'l})$ and the column vector $\boldsymbol{b}=(b_{l'})$ are respectively given by

$$\begin{aligned}
a_{l'l} = {} & \mu_m\langle L^{l'}, \frac{\partial}{\partial r}L^l\rangle + \eta_m\langle L^{l'}, \frac{\partial}{\partial z}L^l\rangle + \sigma_t^g\langle L^{l'}, L^l\rangle + \frac{\alpha_{m+1/2}+\alpha_{m-1/2}}{w_m}\langle L^{l'}, \frac{1}{r}L^l\rangle \\
& + |\mu_m| r_{i+1/2}\langle L_z^{l'}, L_z^l\rangle(\delta_{d1}+\delta_{d3}), \quad if\ l', l\in R, \\
& + |\eta_m|\langle L_r^{l'}, L_r^l\rangle(\delta_{d1}+\delta_{d2}), \quad if\ l', l\in T, \\
& + |\mu_m| r_{i-1/2}\langle L_z^{l'}, L_z^l\rangle(\delta_{d2}+\delta_{d4}), \quad if\ l', l\in L, \\
& + |\eta_m|\langle L_r^{l'}, L_r^l\rangle(\delta_{d3}+\delta_{d4}), \quad if\ l', l\in B, \\
b_{l'} = {} & \frac{(\alpha_{m+1/2}+\alpha_{m-1/2})}{w_m}\sum_{l=1}^{NPT}\psi_{m-1/2}^{gl}\langle L^{l'}, \frac{1}{r}L^l\rangle + \langle L^{l'}, S_m^g\rangle \\
& + |\mu_m| r_{i+1/2}\sum_{\bar{l}\in R}\psi_m^{g\bar{l}}\langle L_z^{l'}, L_z^l\rangle(\delta_{d1}+\delta_{d3}), \quad if\ l'\in R, \\
& + |\eta_m|\sum_{\bar{l}\in T}\psi_m^{g\bar{l}}\langle L_r^{l'}, L_r^l\rangle(\delta_{d1}+\delta_{d2}), \quad if\ l'\in T, \\
& + |\mu_m| r_{i-1/2}\sum_{\bar{l}\in L}\psi_m^{g\bar{l}}\langle L_z^{l'}, L_z^l\rangle(\delta_{d2}+\delta_{d4}), \quad if\ l'\in L, \\
& + |\eta_m|\sum_{\bar{l}\in B}\psi_m^{g\bar{l}}\langle L_r^{l'}, L_r^l\rangle(\delta_{d3}+\delta_{d4}), \quad if\ l'\in B, \\
& (l', l=1\sim NPT).
\end{aligned} \tag{6}$$

Since the matrix $\boldsymbol{A}$ is diagonally dominant, it will not be necessary to use techniques such as the pivoting for solving Eq. (5). Equation (5) is therefore solved with a subroutine based on the simple no-pivoting Crout's method.[10]

2. 4 Other remarks

We describe here some featnres which are specific to our algorithm.

1) Boundary condition for the vacuum right boundary is described by

$$\psi_m^{gl} = 0, \ for\ \mu_m < 0,$$

at any node on the right boundary. Other boundary conditions can be specified similarly.

2) Neutron flows which cross the right boundary of a subregion D_{ij} from the right to the left is calculated with

$$\sum_{\mu_m<0} w_m\mu_m\Big(\sum_{l\in R}\psi_m^{gl}\langle 1, L_z^l\rangle\Big) r_{i+1/2}.$$

Neutron flows across the other boundaries are calculated similarly. These quantities are used for coarse mesh rebalance calculations.

3) Convergence of the inner iteration is judged by the criterion:

$$\max_{ij}\left|1-\frac{\bar{\phi}_{ij}^{p-1}}{\bar{\phi}_{ij}^{p}}\right| < EPSI,$$

where

$$\bar{\phi}_{ij}^{p} = \sum_{l=1}^{NPT} \phi_{00}^{pl} \langle 1, L^{l} \rangle \Big/ \iint_{D_{ij}} r dr dz$$

is an isotropic flux component averaged over D_{ij} in the p-th iteration.

3. Guide to Users' Applications

A schematic flow chart and structure of FFMRZ are given in Figs. 4 and 5. In the figures readers may find a close resemblance to TWOTRAN-II. Apart from the difference in the algorithm used in the program, FEMRZ is based for its structure on TWOTRAN-II. Hence those subroutines with the same names have the same functions as in TWOTRAN-II, though some modifications have been made to adapt to the FEM algorithm. There are, however, several subroutines which have newly been developed for FEMRZ, and some have been deleted from TWOTRAN-II. The new subroutines are as follows, and also indicated in Fig. 5 with.*

IWRITE ; print integer arrays.

NWRITE ; print four dimensional arrays.

PONTER ; point out values from inner product tables.

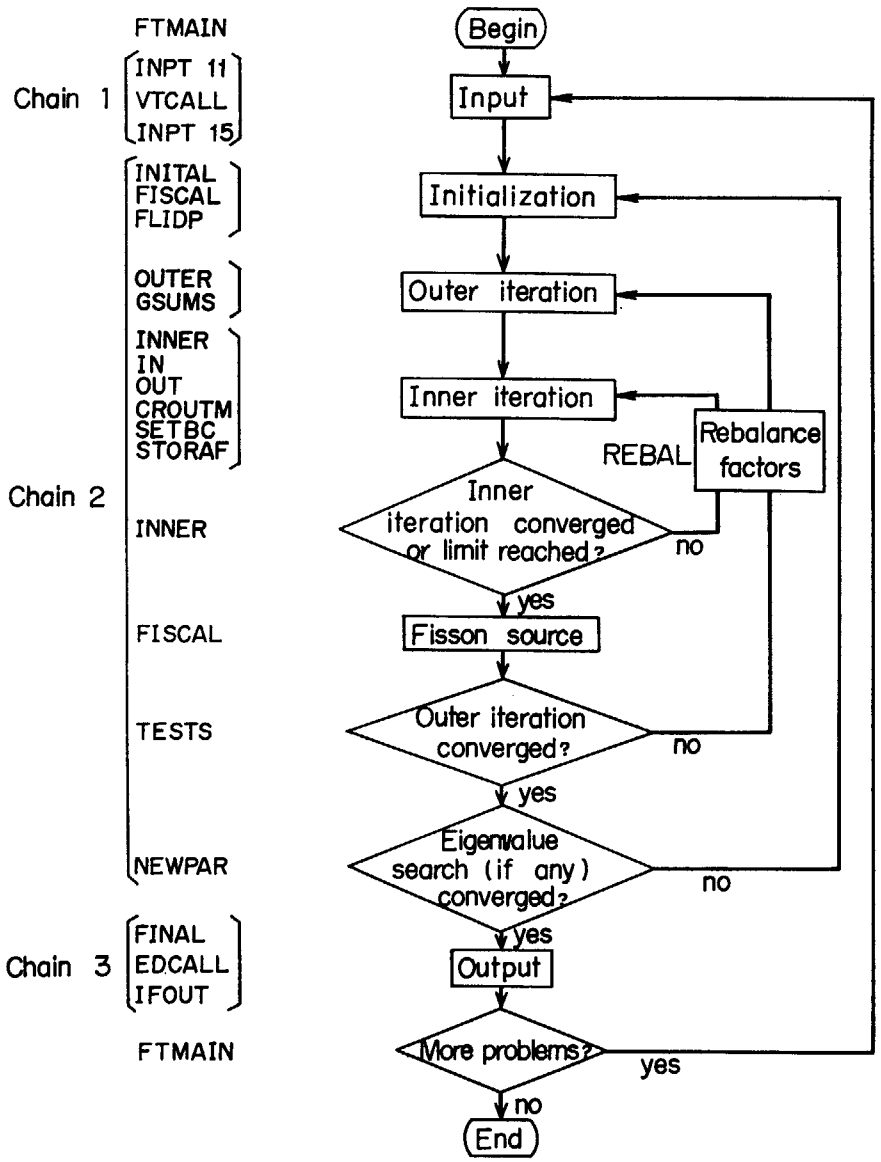

Fig. 4 Program flow and representative subroutines.

VALUE ; calculate inner products.
VTCALL ; prepare for obtaining inner products.
FLIDP ; calculate flux-independent coefficients in Eq. (6).
CROUTM ; solve Eq. (5) by Crout's method.

Major variables which appear in fundamental equations or input descriptions are listed in TABLES 1 and 3. Main files which are necessary for the input and output are summarized in TABLE 2. The FEMRZ requires, in addition, scratch files as seen in Appendix.

The easiest way to know the computer core storage required for a problem is to load the problem in a short-time run. The computation of the core storage is made very early in the execution and the result is printed before most of the data is read.

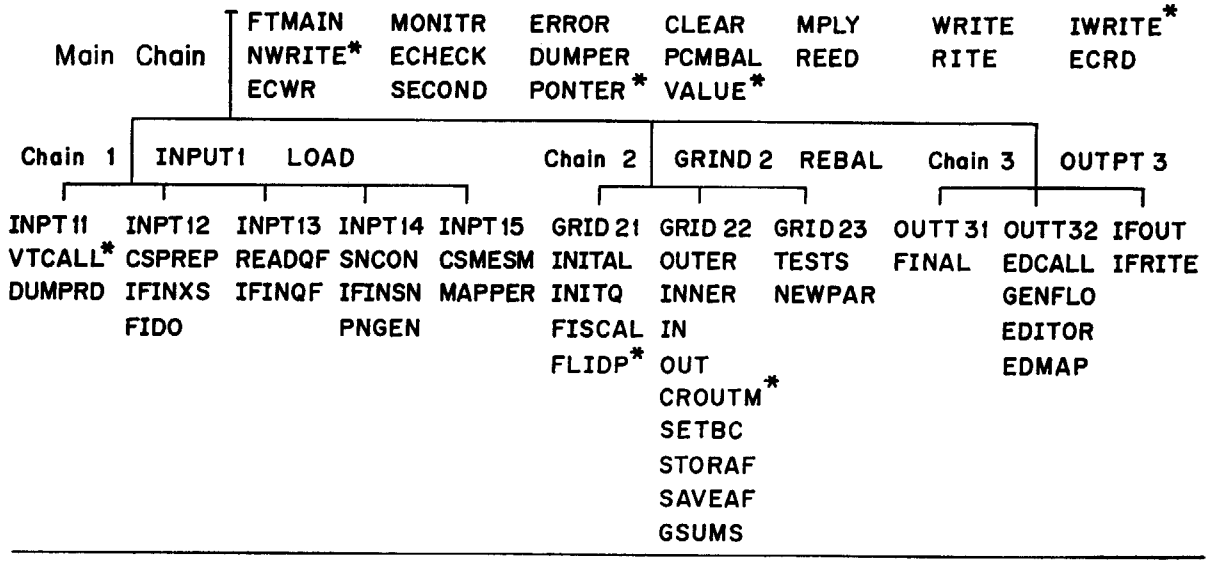

Fig. 5 Program structure.

TABLE 1 Definitions of major variables (see Table 3 for input variables)

Name	Remarks
TIMBDP	Program variable which is defined in FTMAIN to take a periodic dump every *TIMBDP* seconds.
IMP	Sum $IMC+1$
JMP	Sum $JMC+1$
IT	Total number of radial fine mesh intervals
JT	Total number of axial fine mesh intervals
ITP	Sum $IT+1$
JTP	Sum $JT+1$
IP	Sum $IM+1$
JP	Sum $JT+1$
NP	Order of Lagrange's interpolating polynomial
NPP	Sum $NP+1$, number of nodes on a boundary of a subregion
MM	Number of directions per octant
MMT	Number of directions per hemisphere
EPSI	Inner convergence precision set equal to *EPS*
NM	$(ISCT+1)\times(ISCT+2)/2$, number of anisotropic components of flux
NMQ	$(IQAN+1)\times(IQAN+2)/2$, number of anisotropic source components

TABLE 2 Main files used for input and output

Name*	Contents	Remarks
NAFLUX	Binary anglar flux by group generated only on a special last outer interation when requested	The contents for each group consist of 2**JTP* records of length *NPP*IT*MM*2* plus 2**JT* records of length *NPP*ITP* MM*2*.
NDUMP1	Restart dump	This unit is used to make the first restart dump when the problem is not restarted from a previous dump. The unit must contain the restart dump information when the problem is restarted and will then be used to make the second restart dump.
NDUMP2	Restart dump	Second restart dump unit
IAFLUX	Interface form of angular flux	Output of the angular fluxes in interface form is placed on this file for one problem only.
ITFLUX	Interface form of total flux	The code requires that this unit be used when a flux guess is requested from the total flux interface file. The unit is rewound and the records of the first file are used as the input guess. The interface form of the total flux is prepared on this file as problem output.
ISNCON	Interface form of S_n constants	When the file is used as input, only the first one-fourth of the values of weights and direction cosines are read as input. When used as output the file is rewound and written.
IFIXSR	Interface form of source	This file is used only as input for the subregion centered inhomogeneous source. Boundary sources (if any) are obtained from the code dependent input file.
ISOTXS	Interface form of the cross section multi-group file	This file is only used as input when cross sections are requested from an interface file library.

* File name is often read as logical unit.

3. 1 Details of program options

3. 1. 1 Cross sections

The FEMRZ program accepts nuclear cross sections either from the standard file ISOTXS (see TABLE 3), in FIDO format,[13] or in the standard Los Alamos format[12] (see Section 3.2). From the assumption that cross sections are constant in each subregion, the input is made in the same way as in TWOTRAN-II for their mixing, anisotropy and pointwise spatial variation. If the user needs the details, refer to Ref. 12).

3. 1. 2 Mesh spacing

In FEMRZ, the user specifies the domain of the problem according to the following steps as illustrated in Fig. 6.

1) Material coarse mesh is defined by *IMP* r-boundaries (with the variable name of *XRADA*) and *JMP* z-boundaries (*YRADA*) in the respective ascending order.
2) Fine mesh is defined by dividing uniformly each coarse mesh specified in the step 1). The user enters two sets of *IMC* and *JMC* integers (*IHXC* and *IHYC*) indicating the number of fine mesh intervals in each coarse mesh in the r and z direcions, respectively.
3) Rebalance coarse mesh is defined by additional two sets of *IM* and *JM* integers (*IHX* and *IHY*) indicating how many fine mesh intervals are in each rebalance coarse mesh in the respective direction.
4) The user must supply a number (*IDCS*) for each of material coarse mesh zones to designate which cross section block corresponds to the zone.

It would be convenient to specify the rebalance coarse mesh so as to coincide with the material coarse mesh. However, too many rebalance coarse meshes may cause numerical instability and too few may be ineffective for accelerating the convergence. Experiences with TWOTRAN-II and FEMRZ will help to establish optimal coarse mesh strategies.

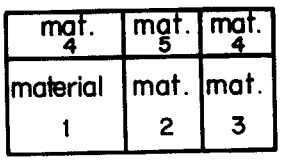

(a) Material coarse meshes and cross section identification numbers

IMC = 3 JMC = 2 (IMC×JMC = 6)

IDCS(1) = 1 IDCS(2) = 2 IDCS (3) = 3
IDCS(4) = 4 IDCS(5) = 5 IDCS (6) = 4

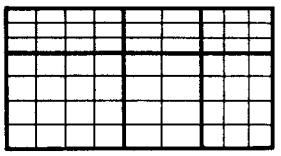

(b) Fine meshes

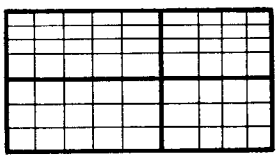

(c) Rebalance coarse meshes

IHXC(1) = 4
IHXC(2) = 2
IHXC(3) = 3
IT = 9

IHYC(1) = 4
IHYC(2) = 3
JT = 7

IM = 2
IHX(1) = 5
IHX(2) = 4

JM = 2
IHY(1) = 3
IHY(2) = 4

Fig. 6 An example of mesh arrangement in a domain.

3. 1. 3 Source options

An anisotropic distributed source $(2_n+1)\ Q^{gl}_{nk}$ in Eq. (3) is entered in the following order:

$(((Q^{gl}_{nkij},\ l=1,\ NPT),\ i=1,\ IT),\ j=1,\ JT),$

for $k=0\sim n,\ n=0\sim IQAN,$

where the order of anisotropy *IQAN* must be at most *ISCT*. In addition, the in-down

boundary sources, for example, is entered in the order given by

$$(((QR1^{gl}_{jm},\ l=1,\ NPP),\ j=1,\ JT),\ m=1,\ MM).$$

They are supplied for each group, from group 1 to group *IGM*.

In addition to $IQOPT=2$ as mentioned above, where the complete array Q^{gl}_{nkij} is entered, there are five options to simplify the reading of Q^{gl}_{nkij}:

IQOPT	Option
0	Q^{gl}_{nkij} is automatically set to zero.
1	Enter an energy spectrum (GR^{g}_{nk}, $g=1$, IGM) for each n and k, in order to have $Q^{gl}_{nkij}=GR_{nk}$ for all i, j and l for each g, n and k.
2	The entire array Q^{gl}_{nkij} is entered in the block of $NPT\times IT\times JT$ continuous numbers for each g, n and k.
3	Enter first a spectrum (GR^{g}_{nk}, $g=1$, IGM) as in option 1. Then enter a spatial shape ($((F_{nkij}$, $l=1$, $NPT)$, $i=1$, $IT)$, $j=1$, $JT)$ in a continuous block of $IT\times JT$ numbers. As a result, $Q^{gl}_{nkij}=GR^{g}F_{nkij}$ for all i, j and l for each g, n and k.
4	Enter a spectrum (GR^{g}_{nk}, $g=1$, IGM), a r-directional spacial shape (X_{nki}, $i=1$, IT), and a z-directional shape (Y_{nkj}, $j=1$, JT). Then, $Q^{gl}_{nkij}=GR^{g}_{nk}X_{nki}Y_{nkj}$ for all i, j and l for each g, n and k.
5	The entire source is read from a standard interface file FIXSRC mounted on unit IFIXSR.

3. 1. 4 Flux options

As is shown below, optinos for reading an input flux guess are similar to those for an input source. They are selected by an integer *ISTART* and the negative value indicates that only the scalar flux is to be read.

ISTART	Option
−5	An entire scalar flux guess RTFLUX (regular flux) or ATFLUX (adjoint flux) is read from standard interface file ITFLUX.
−4	Same as option 4 except that only the istropic components are entered.
−3	Same as option 3 but isotropic components only.
−2	Same as option 2 but isotropic components only.
−1	Same as option 1 but isotropic components only.
0	No flux guess is required, but a fission guess (unity in every subregion) is automatically supplied.
1	As in source option 1, a spectrum is spplied so that $\phi^{gl}_{nkij}=GR^{g}_{nk}$.
2	The entire array ϕ^{gl}_{nkij} is entered in the block of $NPT\times IT\times JT$ continuous numbers for each g, n and k.
3	A spectrum and a shape are entered, so that $\phi^{gl}_{nkij}=GR^{g}_{nk}F_{nkij}$.
4	A spectrum, an i shape and a j shape are entered, so that $\phi^{gl}_{nkij}=GR^{g}_{nk}X_{nki}Y_{nkj}$.
6	A problem-restart dump is read from unit NDUMP1.

3. 1. 5 Flux dumps and restart procedure

Three types of dumps are provided in the same form and each dump may be used to restart a problem. A periodic dump is made every *TIMBDP* seconds in CPU (central processing unit) time. The *TIMBDP* is a program variable set in the main program FTMAIN to meet the processing speed of the computer. A final dump is always made after the suc-

cessful completion of a problem, and a time limit dump is made after a user-specified period time. Dumps are written alternately on unit NDUMP1 and NDUMP2. An output message is written to indicate which unit contains the latest dump.

When the problem execution is continued by using a restart dump, certain input parameters can be changed and edit specifications can be added or modified. It is also possible to use the program to edit a final dump. However, if this option is selected and more information is required to perform the edit, one more outer iteration may be required before performing the edit.

To restart a problem, a special input consisting of three sections is required. The first section is the same as for the normal problem. It is composed of the job title cards and the three integer control cards with the value of *ISTART* set to six shown in TABLE 3. During the restart all other integer values except *ISTART* are ignored. The second section makes use of the namelist feature standard to FORTRAN to permit the user to change some input parameters and enter only those to be changed. The parameters are *IITL, ITLIM, IEDOPT, I2, I4, I6, IANG, IFO, EV, EVM, PV, XLAL, XLAH* and *XLAX*, which are explained in TABLE 3. However, even if no changes are desired, this section cannot be omitted.

The description of namelist block may vary with machine. For the FACOM 230–75 computer (FORTRAN H), an example is shown below.

Column	1 2 3 4 5 6 7 8 9 0 1 2 3 4
Cards	¥ N O C O N V b & T W O I N P b I 2 = 1 , b E V = 0 . 0 & E N D ¥ C O N V

The third section of restart input is the edit section. In FEMRZ, the editing (as well as eigenvalue searches and adjoint computations) is performed in almost the same way as in TWOTRAN-II, and hence the options are described only briefly in TABLE 3. If the user requires details of the options, he may see Ref. 12).

3. 2 Description of input data

As shown in TABLE 3, the input data for FEMRZ are arranged in exactly the order of entrance in the code. They are classified into three categories; 1) job title cards, 2) control numbers and 3) problem dependent data.

With the exception of cross section from the code dependent input file and three edit parameter specifications, all the data of category 3) is loaded with the LASL block loader using the special formats.

These formats are [6(I1, I2, I9)] for reading integers and [6(I1, I2, E9.4)] for floating point numbers. In each word of both of these formats, the first integer field, I1, designates the options listed in TABLE 4. The second integer field, I2, controls the execution of the option, and the remainder of the field, I9 or E9.4, is for the input data. We denote these formats by S(I) for integers and S(E) for floating point numbers.

TABLE 3 Input data cards for FEMRZ

1) Job title cards

Column	Format	Comments
First card 1—6	I6	Number of title or job description cards.
Title cards 1—72	18A4	Title or job description

2) Control numbers

Column	Format	Symbol	Comments
Card 1			
1— 6	I6	ITH	0/1 (direct/adjoint) type of calculation.
7—12	I6	ISCT	0/N (isotropic/N-th order anisotropic) order of scattering calculation. There are not used to compute a scattering source unless some zone material identification number is negative. See *IDCS* below.
13—18	I6	ISN	S_n order. Even integer only. If negative, quadrature coefficients are taken from interface file ISNCON. Otherwise, for $ISN=2$ through 16, built-in constants are used.
19—24	I6	IGM	Number of energy groups.
25—30	I6	IM	Number of rebalance coarse mesh intervals in the r-direction.
31—36	I6	JM	Number of rebalance coarse mesh intervals in the z-direction.
37—42	I6	IBL	Left boundary condition: 0/1=vacuum/reflective.
43—48	I6	IBR	Right boundary condition: 0/1/2=vacuum/reflective/white.
49—54	I6	IBB	Bottom boundary condition: 0/1/2/3=vacuum/reflective/white/periodic.
55—60	I6	IBT	Top boundary condition: 0/1/2/3=vacuum/reflective/white/periodic.
61—66	I6	IEVT	Problem type: 0/1/2/3/4=inhomogeneous source (Q)/k_{eff} calculation/time absorption (alpha) search/nuclide concentration (C) search/zone thickness (delta) search.
67—72	I6	ISTART	Input flux guess and starting options: −5/−4/−3/−2/−1/0/1/2/3/4/6. See section 3.1.4.
Card 2			
1— 6	I6	MT	Total number of materials (cross section blocks including anisotropic components) in the problem.
7— 9	I3	MTPS	Number of input material sets from the interface file ISOTXS. (Caution: each material set from this file yields $ISCT+1$ materials. See *IDLIB* below.)
10—12	I3	MCR	Number of input materials from the code dependent input file. If this number is negative, FIDO format cross sections are read.
13—18	I6	MS	Number of mixture instructions. See items *MIXNUM*, *MIXCOM* and *MIXDEN* below.
19—24	I6	IHT	Row of total cross section in the cross section format. If $IHT<0$, the code assumes that there is no up-scattering in cross section table.
25—30	I6	IHS	Row of within-group scattering cross section in the cross section format.

Column	Format	Symbol	Comments
31—36	I6	IHM	Total number of rows in the cross section format.
37—42	I6	IQOPT	0/1/2/3/4/5: options for input of inhomogeneous source. See Section 3.1.3.
43—48	I6	IQAN	Order of anisotropy of inhomogeneous distributed source.
49—50	I2	IQR	Right boundary source to be specified as input (0/1=no/yes). The source is the value of the incoming flux on the right boundary. See *QR1* and *QR2* below.
51—52	I2	IQB	Bottom boundary source to be specified as input (0/1=no/yes). The source is the value of the incoming flux on the bottom boundary. See *QB1* and *QB2* below.
53—54	I2	IQT	Top boundary source to be specified as input (0/1=no/yes). The source is the value of the incoming flux on the top boundary. See *QT1* and *QT2* below.
55—60	I6	IPVT	0/1/2=none/k_{eff}/alpha parametric eigenvalue entered. See entry *PV* below.
61—66	I6	I ITL	Maximum number of inner iterations allowed per group.
67—72	I6	IXM	0/1 (no/yes). Are the r-direction zone thicknesses to be modified? See entry *XM* below.
Card 3			
1— 6	I6	IYM	0/1 (no/yes). Are the z-direction zone thicknesses to be modified? See entry *YM* below.
7—12	I6	ITLIM	0/seconds. If an integer number of seconds is entered, a restart dump is taken after this number of seconds and then the problem is terminated.
13—18	I6	NPT	Number of node points in a subregion.
19—24	I6	IEDOPT	0/1/2/3/4 (none/option). Edit options. Option 1 is a macroscopic edit and option 2 is a macroscopic plus microscopic edit. Options 3 and 4 give the information of options 1 and 2, respectively, plus a zone relative power density edit. If *IEDOPT* is −1, −2, −3, or −4, an edit will be performed immediately if all necessary data are present. If additional data are needed (e.g. angular fluxes), one outer iteration is performed and then an edit is performed. If *IEDOPT*=−5, direct access to the program output section is provided, for example, to create an output interface file from a final dump.
25—30	I6	ISDF	0/1 (no/yes). Density factor input indicator. See entry *XDF* and *YDF* below.
31	I1	I1	0/1 (no/yes). Full input flux print suppression indicator.
32	I1	I2	0/1/2 (all/isotropic/none). Final flux print indicator.
33	I1	I3	0/1/2 (all/mixed/none). Cross section print indicator.
34	I1	I4	0/1 (yes/no). Final fission print indicator.
35	I1	I5	0/1/2/3 (all/input/normalized/none). Source input print indicator.
36	I1	I6	0/1 (yes/no). Prepare and print balance tables for the rebalance mesh. (Caution: The preparation of these tables requires an additional outer iteration after problem convergence).
37—42	I6	IANG	−1/0/1 (print and store/no/store). Angular flux indicator. The preparation of angular fluxes requires an additional

Column	Format	Symbol	Comments
			outer iteration after problem convergence as well as additional storage.
43—48	I6	IMC	Number of material coarse mesh intervals in the r-direction. The material coarse mesh is the same as the mesh upon which all edits are done. When edits are requested, the angular fluxes must be stored. See entries *IDCS*, *XM*, *IHXC* and *XRADA* below.
49—54	I6	JMC	Number of material coarse mesh intervals in the z-direction.
55—60	I6	IFO	0/1 (no/yes). Interface file output is created. Total (angle-integrated) flux and ISNCON files are always created. Angular flux file is created only if $IANG \neq 0$.
61	I1	IADAF	0/1 (no/yes). Print node-wise angular fluxes.
62	I1	IADFC	0/1 (no/yes). Print node-wise flux components.
Card 4			
1—12	E12.4	EV	Eigenvalue guess. It is satisfactory to enter 1.0 for $IEVT=3$ and 0.0 for all other problems.
13—24	E12.4	EVM	Eigenvalue modifier used only if $IEVT>1$.
25—36	E12.4	PV	Parametric value of k_{eff} for subcritical or supercritical system or for $1/v$ absorption.
37—48	E12.4	XLAL	Lambda lower limit for eigenvalue searches.[12]
49—60	E12.4	XLAH	Search lambda upper limit.
61—72	E12.4	XLAX	Search lambda convergence precision for second and subsequent values of the eigenvalue.
Card 5			
1—12	E12.4	EPS	Convergence precision.
13—24	E12.4	NORM	Normalization factor. Total number of particles in system is normalized to this number, if it is nonzero. No normalization, if *NORM* is zero.
25—36	E12.4	POD	Parameter oscillation damper used in eigenvalue searches.

3) Remaining data

Block name	Format	Number of entries	Comments
IHX	S(I)	IM	Integers defining the number of fine mesh intervals within each rebalance coarse mesh in the r-direction.
IHY	S(I)	JM	Integers defining the number of fine mesh intervals within each rebalance coarse mesh in the z-direction.
IHXC	S(I)	IMC	Integers defining the number of fine mesh intervals within each material coarse mesh in the r-direction.
IHYC	S(I)	JMC	Integers defining the number of fine mesh inservals within each material coarse mesh in the z-direction.
XRADA	S(E)	IMP	Coarse mesh material r-boundaries.
YRADA	S(E)	JMP	Coarse mesh material z-boundaries.
C			Three options are available for reading cross sections. The LASL input format may not be mixed with the FIDO format. 1. LASL input. If *MCR*. GT. 0, *MCR* blocks of

Block name	Format	Number of entries	Comments
			*IHM*IGM* numbers are read in a 6E12.5 format. Each block must be preceded by an identification card read in a 18A4 format. 2. FIDO input. If *MCR*. LT. 0, *MCR* blocks of data are created from FIDO input. FIDO input data must be preceded by 14* (floating point block number 14) loading card. 3. Interface file ISOTXS. When *MTPS*. GT. 0, *MTPS* material sets are read from standard file ISOTXS. On this file, each material set consists of *ISCT*+1 cross section blocks for the isotropic and *ISCT* anisotropic components. The first component of the first material is stored in cross section block *MCR*+1, the first component of the second material is stored in cross section block *MCR*+*ISCT*+2, etc. If the ISOTXS file does not contain *ISCT* anisotropic components, zeroes are supplied for the components not present. If the ISOTXS file contains more components than needed, only the first *ISCT*+1 components are read.
IDLIB	S(I)	MTPS	Position numbers of material sets to be read from ISOTXS. Do not enter unless *MTPS*. GT. 0. The material sets are read in the order specified in this entry, and this order need not be in order of increasing set identification number.
FLUX	S(E)		Input flux guess. Number of entries depends on option controlled by *ISTART*. See Section 3.1.4. Option — Number −5 Input from RTFLUX or ATFLUX standard file −4 *IGM*+*IT*+*JT* −3 *IGM*+*IT*JT* −2 *IGM* blocks of *IT*JT* −1 *IGM* 0 None 1 *NM* sets of *IGM* 2 *IGM* groups of *NM* sets of *IT*JT* 3 *NM* sets of (*IGM*+*IT*JT*) 4 *NM* sets of (*IGM*+*IT*+*JT*) 6 Input from problem-restart dump
Q	S(E)		Input source. Number of entries depends on option controlled by *IQOPT*. See Section 3.1.3. Option — Number 0 None 1 *NMQ* sets of *IGM* 2 *IGM* groups of *NMQ* blocks of *NPT*IT*JT* 3 *NMQ* sets of (*IGM*+*NPT*IT*JT*) 4 *NMQ* sets of (*IGM*+*IT*+*JT*) 5 Input from standard file FIXSRC

Block name	Format	Number of entries	Comments
QR1	S(E)	NPP*JT*MM	Right boundary source (flux) in the in-down directions. Do not enter unless $IQR=1$.
QR2	S(E)	NPP*JT*MM	Right boundary source (flux) in the in-up directions. Do not enter unless $IQR=1$.
QB1	S(E)	NPP*IT*MM	Bottom boundary source (flux) in the in-up directions. Do not enter unless $IQB=1$.
QB2	S(E)	NPP*IT*MM	Bottom boundary source (flux) in the out-up directions. Do not enter unless $IQB=1$.
QT1	S(E)	NPP*IT*MM	Top boundary source (flux) in the in-down directions. Do not enter unless $IQT=1$.
QT2	S(E)	NPP*IT*MM	Top boundary source (flux) in the out-down directions. Do not enter unless $IQT=1$.
IDCS	S(I)	IMC*JMC	Cross section zone identification numbers. These numbers assign a cross section block to each zone defined by the material coarse mesh. If these numbers are negative, an anisotropic scattering source is calculated in the zone, but the numbers need not be negative when $ISCT>0$.
CHI	S(E)	IGM	Fission fractions. Fraction of fission yield emerging in each group.
VEL	S(E)	IGM	Group speeds. Used only in time absorption calculations.
MIXNUM	S(I)	MS	Numbers identifying cross section block being mixed. Do not enter if $MS=0$.
MIXCOM	S(I)	MS	Numbers controlling cross section mixture process. Do not enter if $MS=0$.
MIXDEN	S(E)	MS	Mixture densities. Do not enter if $MS=0$.
XM	S(E)	IMC	Material r-mesh modification factors. Do not enter unless $IEVT=4$ and $IXM>0$.
YM	S(E)	JMC	Material z-mesh modification factors. Do not enter unless $IEVT=4$ and $IYM>0$.
XDF	S(E)	IT	Radial fine mesh density factors. Do not enter if *ISDF*. EQ. 0.
YDF	S(E)	JT	Axial fine mesh density factors. Do not enter if *ISDF*. EQ. 0. The effective cross section in a subregion D_{ij} is that for the point defined by the *IDCS* array multiplied by the factor XDF(i)*YDF(j).
NEDS	I6	1	Integer defining number of edits to be performed. Do not enter unless $0<\|IEDOPT\|<5$.
MN	I6	1	Integer defining number of microscopic activities to be computed. Do not enter unless $\|IEDOPT\|=2$ or 4.
MICID	S(I)	MN	Integers defining material blocks for which microscopic edit is to be made (for $IEDOPT=2$ and 4 only).
NZ, NORMZ	2I6	2	The integer *NZ* is the number of edit zones. The integer *NORMZ* is the zone to which the power

Block name	Format	Number of entries	Comments
NEDZ	S(I)	IMC*JMC	density is normalized (*NORMZ* is not used unless *IEDOPT*=3 or 4). Integers defining which edit zone each coarse mesh material zone is in. The edit blocks beginning with *NZ*, *NORMZ* must be repeated *NEDS* times. Do not enter these cards unless $0<\|IEDOPT\|<5$.

TABLE 4 Options for special read formats[12]

Value of I1	Nature of option
0 or blank	No action
1	Repeat 9 field value by the number of times indicated in I2 field.
2	Place the number of linear interpolants indicated in I2 field between 9 field value and the next value. (Not allowed for integers.)
3	Terminate reading of data block. A 3 must follow last data word of all blocks.
4	Fill the remainder of block with 9 field value. This operation must be followed by a terminate (3).
5	Repeat 9 field value by 10 times the value in the I2 field.
9	Skip to next data card.

4. Some Examples and Discussions

To demonstrate the performance of FEMRZ, several examples, including real scale problems, were calculated and are shown in this chapter. The results are also compared with those by TWOTRAN-II for reference.

Example 1: This problem is to obtain the eigenvalue (effective multiplication factor) of a nuclear reactor with a simple geometry for various numbers of subregions. The reactor configuration is shown in Fig. 7 and the input data for the case of $IT=2$, $JT=2$ and $NPT=9$ is given in Appendix.

It is shown in Fig. 8 that the solution of biquadratic approximation ($NP=2$) converges faster than that of diamond difference scheme in the similar computing condition. In the course of FEM calculations, the negative fluxes appeared in some nodes in the early stage of calculations, but no recipe for correcting the values was needed for the convergences.

Example 2: This problem is for a large fast reactor illustrated in Fig. 9. We show in Fig. 10 the solution of the isotropic componont of the first group flux along the radial direction indicated in Fig. 9.

It may be natural that the coarse mesh solution obtained from TWOTRAN-II can not well represent the correct profile. In addition, uneven coarse mesh calculations may fail to converge. The FEMRZ generally requires more computing cost than TWOTRAN-II to obtain the solution of the same order of accuracy, but we can use it without considering about the adequacy of sizes of subregions.

Example 3: This reactor system, shown in Fig. 11, is taken up to examine the feature of discontinuity at the material boundary where the flux changes steeply. The cross section are given in TABLE 5.

As shown in Fig. 12, the continuous solution of TWOTRAN-II at the B_4C control rod-core boundary is bounded from above and below by the discontinuous solutions of FEMRZ. Such discontinuities are seen only in the very vicinity of the boundary.

Example 4: As stated in Chapter 1, FEMRZ can solve not only eigenvalue problems but also other problems. As an example, a fixed source problem is shown here. The con-

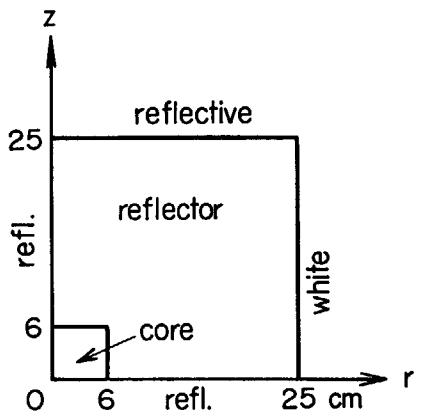

Fig. 7 A reactor configuration and boundary conditions for P_0, S_4, 3-energy-group sample calculations (Example 1).

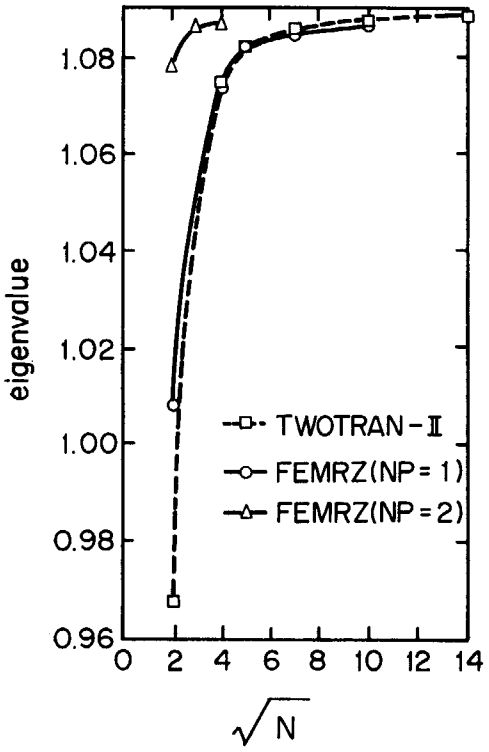

Fig. 8 Dependencies of the eigenvalues obtained by FEM and S_n methods on the number of subregions N for Example 1.

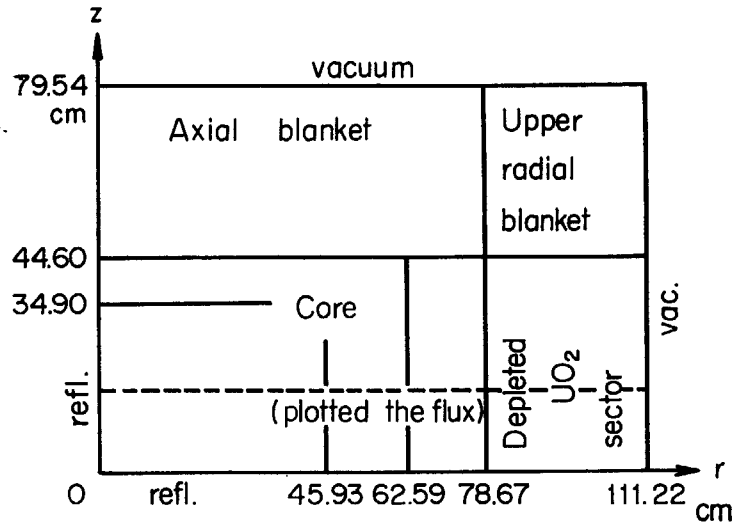

Fig. 9 A fast reactor configuration and boundary conditions for P_1, S_4, 3-energy-group sample calculations (Example 2).

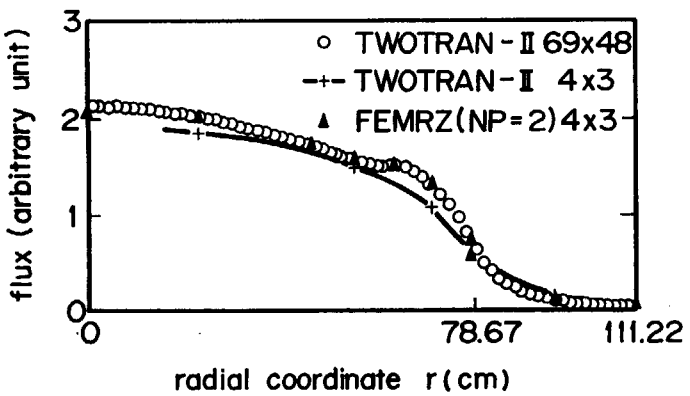

Fig. 10 Comparison of the first group scalar fluxes along the radial direction indicated in Fig. 9 for Example 2.

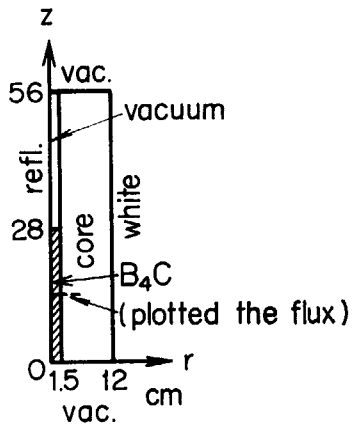

Fig. 11 A reactor configuration containing a control rod and boundary conditions for P_0, S_4, 2-energy-group sample calculations (Example 3).

TABLE 5 Cross sections (cm^{-1}) used for Example 3 (see Fig. 11)

Material	B_4C		Core	
Group	1	2	1	2
$\sigma_{n,2n}$	4.50×10^{-6}		1.90×10^{-5}	
σ_{tr}	3.24×10^{-1}	1.05×10^{1}	3.27×10^{-1}	1.30×10^{-2}
σ_a	2.59×10^{-2}	1.29×10^{1}	7.21×10^{-3}	1.19×10^{-1}
$\nu\sigma_f$			4.74×10^{-3}	2.00×10^{-1}
σ_t	3.24×10^{-1}	1.05×10^{1}	3.27×10^{-1}	1.30
σ_{gg}	2.98×10^{-1}	-2.44	2.84×10^{-1}	1.18
$\sigma_{g-1,g}$		7.60×10^{-22}		3.58×10^{-2}

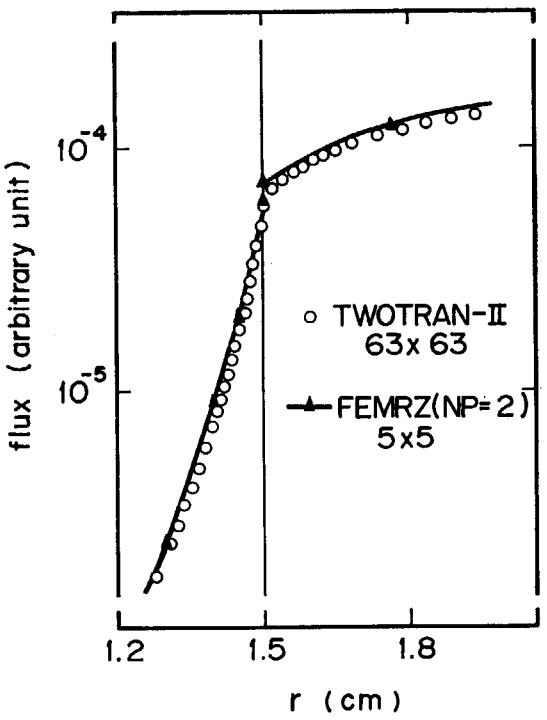

Fig. 12 Second group scalar fluxes in the neighborhood of the control rod along the line indicated in Fig. 11 for Example 3.

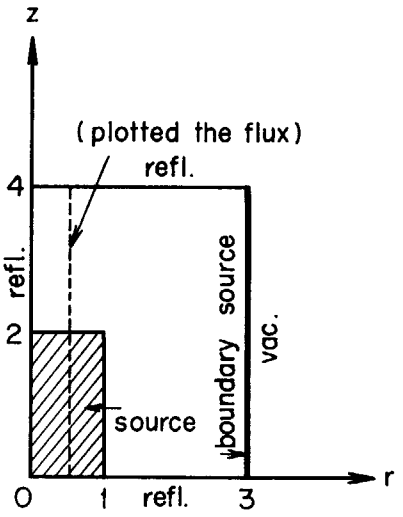

Fig. 13 A homogeneous reactor configuration with fixed sources and boundary conditions for P_0, S_4, 1-energy-group sample calculations (Example 4).

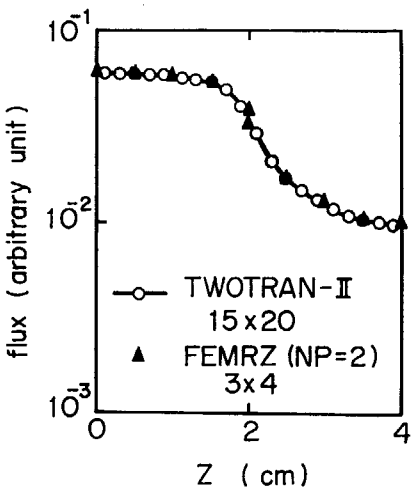

Fig. 14 Scalar fluxes along the axial direction indicated in Fig. 13 for Example 4.

figuration of the system and the computing conditions are showe in Fig. 13. The solutions of the scalar flux along the axial direction indicated in Fig. 13 are shown in Fig. 14. The solution obtained with FEMRZ fits well with the fine mesh solution of TWOTRAN-II.

5. Conclusions

We have developed a new computer program FEMRZ for solving neutron transport problems in (r,z) cylindrical geometry by the use of the finte element method. Several test calculations are compared with the results obtained with a diamond difference S_n program TWOTRAN-II, on which the main flow of our program is based.

The results have shown that the discontinuous method in the biquadratic approximation of FEMRZ gives an accurate and stable solution even with coarse mesh calculations. However, FEMRZ requires more computer core storage and computing time compared with those for TWOTRAN-II which has highly been optimized for both features. It is hoped that FEMRZ will be improved to be more efficient through an accumulation of the application experiences.

Acknowledgements

We are much indebted to Dr. T. Asaoka for his valuable discussions. We are also thankful to Mr. T. Ise for his many beneficial advices.

References

1) Zienkiewicz O. C. and Cheung, Y. K. : "The Finite Element Method in Structural and Continuum Mechanics," McGraw-Hill Book Co. Inc., New York, N. Y. (1967)
2) For example, Strang G. and Fix G. J. : "An Analysis of the Finite Element Method," Prentice-Hall (1973)
3) Ohnishi T. : "Application of Finite Element Solution Technique to Neutron Diffusion and Transport Equations," Proceedings of Conference on New Developments in Reactor Mathematics and Applications, Idaho Falls, Idaho (1971)
4) Reed W. H., Hill T. R., Brinkley F. W. and Lathrop K. D. : "TRIPLET : A Two-Dimensional, Multi-group, Triangular Mesh, Planar Geometry, Explicit Transport Code," LA-5428-MS (1973) or Reed W. H. and Hill T. R. : "Triangular Mesh Methods for Neutron Transport Equation," CONF 730414, I-10 (1973)
5) Froehlich R. : "Current Problems in Multidimensional Reactor Calculations," CONF 730414, VII-1 (1973)
6) Miller W. F. Jr., Lewis E. E. and Rossow E. C. : "The Application of Phase-Space Finite Elements to the One-Dimensional Neutron Transport Equation," *Nucl. Sci. Eng.*, **51**, 148 (1973)
7) Miller W. F. Jr., Lewis E. E. and Rossow E. C. : "The Application of Phase-Space Finite Elements to the Two-Dimensional Neutron Transport Equation in X-Y Geometry," *Nucl. Sci. Eng.*, **52**, 12 (1973)
8) Horikami K., Nakahara Y., Fujimura T. and Ohnishi T. : "Finite Element Method for Solving Neutron Transport Problems in Two-Dimensional Cylindrical Geometry," JAERI-M 5793 (1974)
9) Fujimura T., Ohnishi T., Tsutsui T., Horikami K. and Nakahara Y. : "Application of Finite Element Method to Two-Dimensional Multi-Group Neutron Transport Equation in Cylindrical Geometry," *J. Nucl. Sci. Technol*, **14**, 541 (1977)

10) Westlake J. R. : "A Handbook of Numerical Matrix Inversion and Solution of Linear Equation," John Wiley & Sons, Inc., New York, N. Y. (1968)
11) Nakahara Y. and Fujimura T. : "Convergence Acceleration Algorithms of the Iterative Methods Used in Nuclear Reactor Analysis Codes," JAERI-M 5590 (1974) (in Japanese)
12) Lathrop K. D. and Brinkley F. W. : "TWOTRAN-II : An Interfaced, Exportable Version of the TWOTRAN Code for Two-Dimensional Transport," LA-4848-MS (1973)
13) Engle W. W. Jr. : "A Users Manual for ANISN, A One Dimensional Discrete Ordinates Transport Code with Anisotropic Scattering," K-1693 (1967)

Appendix : Input Setup for Example 1

```
....*....1....*....2....*....3....*....4....*....5....*....6....*....7....*....8

¥NO       N999,                                                          /
                                                                       P,0/PCH     0
                                                                       W,0/PAGE   40
                                                                       C,1/CORE   64
                                                                       T,4/TIME   5M
#GJOB     1142309,FUJIMURA,T,446,01                                      /FEMRZ
#HFORT
      COMMON /FWBGN1/ IDUSE(18),LAST,LASTEC,IGCDMP,IPSO,LTSO,IPFL,LTFL, 00000500
     1IPFX,LTFX,LXFX,IPXS,IPXSCT,LTXS,LTOXS,LTAXS,IP@S,LT@S,IEREC,I2,I4,00000600
     216,ISPAN@,IPHAF,IPVAF,LTHAF,LTVAF,IFO                             00000700
      COMMON /FWBGN2/ TIMBDP,TIMSLD,TIMOFF,MAXLEN,MAXECS,LENMCB,LENCIA, 00000800
     1IFNOVY,IRCOVY,I1,I3,I5                                            00000900
      COMMON /LOCAL/ NERROR,ITLIM,ISNT,MCR,MTP,MTPS,NISOXS,LMTP,IEDOPS, 00001000
     1NEXTER,JFISC,IEDIT(2),LIMIT,LENCLR                                00001100
      COMMON /SWEEP/ BA,BC,J,J1,J2                                      00001200
      COMMON /UNITS/ NINP,NOUT,NAFLUX,NDUMP1,NDUMP2,NEXTRA,NEDIT,IAFLUX,00001300
     1ITFLUX,ISNCON,IFIXSR,ISOTXS                                       00001400
      COMMON IA(300),A(28000)
      EQUIVALENCE (IA(197),TIN),(IA(247),TIMACC)                        00001700
      REWIND 3
      REWIND 17
      REWIND 18
      REWIND 40
      REWIND 30
      REWIND 31
      REWIND 32
      REWIND 8
      REWIND 9
      REWIND 33
      REWIND 34
      MAXLEN=28000
      LENMCB=45                                                         00002200
      LENCIA=300
      NINP = 5                                                          00002700
      NOUT = 6                                                          00002800
      NEDIT=17                                                          00002900
      NEXTRA=18                                                         00003000
      NAFLUX = 3                                                        00003100
      ITFLUX=30                                                         00003600
      IAFLUX=31                                                         00003700
      ISNCON=32                                                         00003800
      IFIXSR=33                                                         00003900
      ISOTXS=34                                                         00004000
  100 CONTINUE                                                          00004400
      NDUMP1 = 8                                                        00004800
      NDUMP2 = 9                                                        00004900
      CALL REED (NDUMP1,0,0,0,0,4)                                      00005300
      CALL REED (NDUMP2,0,0,0,0,4)                                      00005400
      CALL REED (NEDIT,0,0,0,0,4)                                       00005500
      CALL RITE (NEDIT,0,0,0,0,4)                                       00005600
      TIMBDP=600.
      CALL SECOND (TIMSLD)                                              00006100
      IGCDMP=0                                                          00006200
      NERROR=0                                                          00006300
      NEXTER=0                                                          00006400
```

```
....*....1....*....2....*....3....*....4....*....5....*....6....*....7....*....8

      CALL INPUT1                                                          00006800
      CALL GRIND2                                                          00007200
      CALL OUTPT3                                                          00007600
      T=TIN                                                                00007700
      CALL SECOND (TIN)                                                    00007800
      T=(TIN-T+TIMACC)/60.0                                                00007900
      WRITE (NOUT,110)T                                                    00008000
      GO TO 100                                                            00008400
  110 FORMAT (1H0//////41H0***** TOTAL EXECUTION TIME IN MINUTES = 1PE1200023000
     1,4)                                                                  00023100
      END                                                                  00023200
*HLIED  J2309,FEMRZ,B=MAP,SIMPL=OVLY,RBSPC=99,DIRCT=77
SGMT  MAIN
SELECT   (FTMAIN,MONITR,ERROR,CLEAR,MPLY,WRITE,IWRITE,NWRITE,          /
        ECHECK,DUMPER,PCMBAL,                                          /
          REED,RITE,ECRD,ECWR,SECOND,DATE1,PONTER,VALUE)
SGMT  LINK1,CHN=MAIN
SELECT    (INPUT1,LOAD)
SGMT  LINK11,CHN=LINK1
SELECT   (INPT11,VTCALL,DUMPRD)
SGMT  LINK12,CHN=LINK1
SELECT    (INPT12,CSPREP,IFINXS,FIDO)
SGMT  LINK13,CHN=LINK1
SELECT    (INPT13,READ@F,IFIN@F)
SGMT  LINK14,CHN=LINK1
SELECT    (INPT14,SNCON,IFINSN,PNGEN)
SGMT  LINK15,CHN=LINK1
SELECT    (INPT15,CSMESH,MAPPER)
SGMT  LINK2,CHN=MAIN
SELECT    (GRIND2,REBAL)
SGMT  LINK21,CHN=LINK2
SELECT    (GRID21,INITAL,INIT@,FISCAL,FLIDP)
SGMT  LINK22,CHN=LINK2
SELECT   (GRID22,OUTER,INNER,IN,OUT,CROUTM,FIXUP,                      /
          SETBC,STORAF,SAVEAF,GSUMS)
SGMT  LINK23,CHN=LINK2
SELECT    (GRID23,TESTS,NEWPAR)
SGMT  LINK3,CHN=MAIN
SELECT    (OUTPT3)
SGMT  LINK31,CHN=LINK3
SELECT   (OUTT31,FINAL)
SGMT  LINK32,CHN=LINK3
SELECT    (OUTT32,EDCALL,GENFLO,EDITOR,EDMAP)
SGMT  LINK33,CHN=LINK3
SELECT    (IFOUT,IFRITE)
FIN
*HRUN
*DISK  F03
*DISK  F17
*DISK  F18
*DISK  F40
*DISK  F30
*DISK  F31
*DISK  F32
*DISK  F08
```

```
....*....1....*....2....*....3....*....4....*....5....*....6....*....7....*....8

*DISK  F09
*DISK  F33
*DISK  F34
*DATA
     3
 FEMRZ   EXAMPLE 1
 P0,S4,3-GROUP CALCULATION
 B.C. =1211
     0      0      4      3      2      2      1      2      1      1      1    -1INT    1
     4      2      8      3      4      6      0      0      0      0     10     0INT    2
     0    240      9      0      0000000      0      2      2    000             INT    3
   0,0           0,0           0,0           0,05          0,5           0,01    REAL   1
    1,0  - 3      1,0           1,0                                             REAL   2
1 2           13                                                               REB F. R
1 2           13                                                               REB F. Z
1 2           13                                                               MAT F. R
1 2           13                                                               MAT F. Z
    0,0           6,0           25,0     3                                     RADI   R
    0,0           6,0           25,0     3                                     AXI    Z
 TEST CROSS SECTIONS FOR ELEMENT NUMBER 1 BY GROUP.
  1,35          3,25          4,55          1,8                 0,0           0,0    EL1GP1
 1,45          3,075         5,2           3,3           1,05          0,0           EL1GP2
 2,05          4,25          9,5           7,45          0,45          0,35          EL1GP3
 TEST CROSS SECTIONS FOR ELEMENT NUMBER 2 BY GROUP.
 0,6           1,35          4,45          1,9           0,0           0,0           EL2GP1
 0,15          0,05          5,0           4,25          1,5           0,0           EL2GP2
   0,3           0,0           9,5           9,2           0,6           0,45          EL2GP3
   0,56          0,341         0,099    3                                          FLUX 3GD
1 1           31 3          43                                                    REGION
   0,56          0,341         0,099    3                                          CHI  3GD
   22,19         12,5          5,599    3                                          VEL  3GD
104           3104          43                                                    NUM  3GD
              0             1             2             0             0           1COM 3GD
              2             03                                                    COM  3GD
   0,0           0,94          0,06          0,048         0,0           0,007     DEN  3GD
   0,993         0,048    3                                                       DEN  3GD
¥JEND
```